Available online at www.sciencedirect.com
ScienceDirect
Ceramics International 37 (2011) 341–347
CERAMICS INTERNATIONAL
www.elsevier.com/locate/ceramint

Phase transformation kinetics of 3 mol% yttria partially stabilized zirconia (3Y-PSZ) nanopowders prepared by a non-isothermal process

Chih-Wei Kuo [a], Yun-Hwei Shen [a], Shaw-Bing Wen [b], Huey-Er Lee [c], I.-Ming Hung [d], Hong-Hsin Huang [e], Moo-Chin Wang [f,*]

[a] Department of Resources Engineering, National Chen Kung University, 1 Ta-Hsueh Road, Tainan 70101, Taiwan
[b] General Education Center, Meiho Institute of Technology, 23 Pingkuang Road, Neipu, Pingtung 91202, Taiwan
[c] Faculty of Dentistry, Kaohsiung Medical University, 100 Shih-Chuan 1st Road, Kaohsiung 80708, Taiwan
[d] Department of Chemical Engineering and Materials Science, Yuan Ze University, 135 Yuandong Rd., Jhongli City, Taoyuan County 320, Taiwan
[e] Department of Electrical Engineering, Cheng Shiu University, 840 Cheng Ching Road, Niaosong, Kaohsiung 83347, Taiwan
[f] Department of Fragrance and Cosmetic Science, Kaohsiung Medical University,100 Shih-Chuan 1st Road, Kaohsiung 80708, Taiwan

Received 13 July 2009; received in revised form 12 June 2010; accepted 30 August 2010
Available online 29 September 2010

Abstract

A crystalline nanopowder of 3 mol% yttria-partially stabilized zirconia (3Y-PSZ) has been synthesized using $ZrOCl_2$ and $Y(NO_3)_3$ as raw materials throughout a co-precipitation process in an alcohol–water solution. The phase transformation kinetics of the 3Y-PSZ freeze dried precursor powders have been investigated by nonisothermal methods. Differential thermal and thermogravimetric analyses (DTA/TG), X-ray diffraction (XRD), scanning electron microscopy (SEM), transmission electron microscopy (TEM) and high resolution TEM (HRTEM) have been utilized to characterize the 3Y-PSZ nanocrystallites. When the 3Y-PSZ freeze dried powders are calcined in the range of 703–1073 K for 2 h, the crystal structure is composed of tetragonal and monoclinic ZrO_2. The BET specific surface area of the 3Y-PSZ freeze dried precursor powders calcined at 703 K for 2 h is 118.42 m^2/g, which is equivalent to a crystallite size of 8.14 nm. The activation energy from tetragonal ZrO_2 converted to monoclinic ZrO_2 in the 3Y-PSZ freeze dried precursor powders was determined as 401.89 kJ/mol. The tetragonal (T) and monoclinic (M) ZrO_2 phases coexist with a spherical morphology, and based on TEM examination have a size distribution between 10 and 20 nm. When sintering green compacts of the 3Y-PSZ, a significant linear shrinkage of 8% is observed at about 1283 K. On sintering the densification cycle is complete at approximately 1623 K when a total shrinkage of 32% is observed and a final density above 99% of theoretical was achieved.

Keywords: 3Y-PSZ; Non-isothermal sintering; Phase transformation kinetics; Grain size

1. Introduction

Pure zirconia (ZrO_2) is the only metal oxide that has acidity and basicity as well as reducing and oxidizing ability. It undergoes at least three crystallographic transformations (monoclinic, tetragonal and cubic) when it cools from high temperature to room temperature. Zirconia-based ceramics have been used for advanced and structural applications. The usage of these solids as catalysts and solid electrolytes [1] in high-temperature electrochemical devices and the possibility that the microstructure of materials can be designed and optimized justify the interest with regard to pure and doped zirconia. Stabilized ZrO_2 solid solution has been used widely in several commercial fields including fuel cells, oxygen sensors and high-temperature pH sensors, and so on [2]. Among stabilized systems, yttria-stabilized zirconia (YSZ) is the most common. YSZ has high ionic conductivity and thermal stability, for which it is used in oxygen sensors and for the electrolytes in solid oxide fuel cells (SOFC) [1].

The crystal structure of ZrO_2, with appropriate cooling, can be retained at room temperature as tetragonal with the addition of about 3 mol% Y_2O_3, while Y_2O_3 additions up to 8 mol% promote phase stabilization of the cubic form at room temperature [3]. To avoid phase transformation during the heating and cooling cycles, YSZ ceramics with a single cubic phase are desirable for high temperature applications [4]. When

* Corresponding author. Tel.: +886 7 3121101x2366; fax: +886 7 3210683.
E-mail address: mcwang@kmu.edu.tw (M.-C. Wang).

0272-8842/$36.00
doi:10.1016/j.ceramint.2010.09.018

doped with yttria, fine-grained tetragonal zirconia polycrystals (Y-TZP) and partially stabilized zirconia (Y-PSZ) exhibit excellent strength and fracture toughness because of the stress-induced martensitic phase transformation of tetragonal to monoclinic symmetry [5].

The thermal behavior of various materials has been investigated by a DTA technique. For the crystallization and phase transition study of materials, DTA is useful in determining the transition temperature. A number of authors have provided detailed kinetic analyses by a DTA method in which crystallization and crystal growth mechanisms can be elucidated [6,7].

In the present study, $ZrOCl_2{\cdot}8H_2O$ and $Y(NO_3)_3{\cdot}6H_2O$ have been used for the synthesis of YSZ nanocrystallites via a coprecipitation and calcination process. Differential thermal and thermogravimetric analyses (DTA/TG), X-ray diffractometry (XRD), scanning electron microscopy (SEM), transmission electron microscopy (TEM), electron diffraction (ED) and dilatometric analyzer (DA) have been utilized to characterize the phase transformation behavior of the 3Y-PSZ precipitates and green compacts.

The purposes of this study are (i) to evaluate the thermal behavior of the 3Y-PSZ freeze dried precursor powders, (ii) to study the phase transformation behavior of the 3Y-PSZ freeze dried precursor powders, (iii) to observe the microstructure and morphology of the 3Y-PSZ freeze dried precursor powders after calcination and (iv) to evaluate the sintering curves of the 3Y-PSZ powders.

2. Experimental

2.1. Sample preparation

The starting materials were zirconyl chloride ($ZrOCl_2{\cdot}8H_2O$) and yttrium nitrate [$Y(NO_3)_3{\cdot}6H_2O$]. Zirconyl chloride and yttrium nitrate were dissolved in a deionized water and ethanol solution of a volume ratio of 1:5. The ratio of Y_2O_3 to ($Y_2O_3 + ZrO_2$) equal to 3 mol% in solution was prepared and labeled as 3Y-PSZ. The mixed solution was then added with a specific amount of polyethylenglycol (PEG) as a dispersant because 0.06 wt% of PEG can greatly decrease agglomeration. The mixed solution was stirred and heated in a thermostatic bath and held at 348 K for 2 h to obtain white precipitates. NH_4OH was then added into the sol bath until a pH 9 was attained. After precipitation, the precipitates were repeatedly rinsed and filtered with a large amount of deionized water and tested with $AgNO_3$ solution to ensure no AgCl precipitation occurred. Subsequently, precipitates were freeze-dried at 218 K in a vacuum. Finally, the freeze dried powders were calcined at 673–1073 K for 2 h.

The green compact samples were pre-shaped using a uniaxial press at a pressure of 40 MPa then cold isostatically pressed at 98 MPa. The density of the sintered samples was measured using Archimedes' method [8].

2.2. Sample characterization

The crystalline phases were identified using an X-ray diffractometer (XRD, Model Rad IIA, Rigaku, Tokyo) with Cu Kα radiation and an Ni filter, operating at 30 kV, 20 mA and a scanning rate of 0.25°/min.

The crystallite size of tetragonal and monoclinic ZrO_2 calcined powders were calculated from the XRD data using Scherrer's equation [9]:

$$d = \frac{0.9\lambda}{\beta \cos\theta} \tag{1}$$

where d is the crystallite sizes of the tetragonal or monoclinic ZrO_2 phase, $\lambda = 1.5405$ Å is the wavelength of Cu Kα radiation, β is the full width at half maximum (FWHM) intensity in radians. The $(1\ 0\ 1)_T$ and $(\bar{1}\ 1\ 1)_M$ reflections at $2\theta = 30.1$ and 28.1° were used to define the FWHM intensity of tetragonal and monoclinic ZrO_2, respectively, within the various crystalline phases.

The specific surface area of the powders was obtained by the BET method, and the measured surface area was converted to the equivalent particle size using the following equation [10]:

$$d_{BET} = \frac{\kappa}{\rho S_{BET}} \tag{2}$$

where d_{BET} is the average particle size, κ is the shape coefficient (close to a spherical shape, $\kappa = 6$), S_{BET} is the specific surface area expressed in m^2/g, and $\rho = 6$ is the theoretical density of the YSZ in g/cm^3.

The sintering curves of 3Y-PSZ freeze dried powders calcined at 773 K for 2 h were studied by a dilatometric analyzer (DA, Setsys evolution, Setaram) with a heating rate of 5 K/min from room temperature to 1673 K. Samples for dilatometric tests were cut from the pressed disk and shaped into a bar of 20 mm × 2 mm × 2 mm. Sintering was performed in an alumina tube furnace containing an alumina push rod. The push rod applied a maximum pressure of 414 Pa to the sample during sintering.

The final fired density of the sintered compact was then calculated according to the green density and the measured linear shrinkage. The density was also determined by the Archimedes' method using distilled water as the medium.

The morphology of the Au-coated-calcined 3Y-PSZ nanocrystallite powders was examined by scanning electron microscopy (SEM, Philips, XL-40FEG) and transmission electron microscopy (TEM, H700H, Hitachi) operating at 200 kV. Electron diffraction (ED) was utilized to confirm the phases of the calcined 3Y-PSZ nanocrystallite powders, and high resolution TEM (HRTEM) examination was also made for the calcined sample.

3. Results and discussion

3.1. Thermal behavior, phase identification and stability of 3Y-PSZ freeze dried precursor powders

Fig. 1 illustrates the XRD patterns of the 3Y-PSZ freeze dried precursor powders calcined at different temperatures in the range 623–1073 K for 2 h. The XRD pattern of the 3Y-PSZ freeze dried precursor powders calcined at 623 K for 2 h is shown in Fig. 1(a), and reveals that the calcined powders are

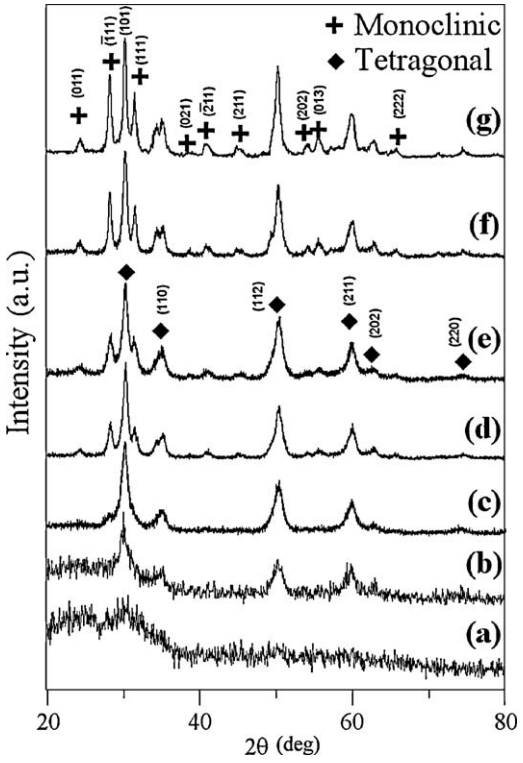

Fig. 1. XRD patterns of 3Y-PSZ freeze dried precursor powders calcined at different temperatures for 2 h: (a) 623 K, (b) 673 K, (c) 703 K, (d) 773 K, (e) 873 K, (f) 973 K and (g) 1073 K.

still almost amorphous. Fig. 1(b) shows the 3Y-PSZ freeze dried powders when calcined at 673 K for 2 h, and indicates that the crystalline phase is the tetragonal ZrO_2 phase of poor crystallinity or small crystallite size [11]. This result corresponds to the DTA curve of Fig. 3(a) and shows that the tetragonal ZrO_2 starts transforming at 673 K. The XRD pattern of the 3Y-PSZ freeze dried precursor powders calcined at 703 K for 2 h is shown in Fig. 1(c), and indicates the initial appearance of the monoclinic $(\bar{1}\,1\,1)_M$ peak. The $(\bar{1}\,1\,1)_M$ reflection is very weak and broad, indicating poor crystallinity or very small crystallite size [11]. Moreover, the crystallinity of the tetragonal phase content and size in Fig. 1(c) is suddenly increased beyond that shown in Fig. 1(b). The 3Y-PSZ freeze dried precursor powders calcined at 773–1073 K for 2 h are shown in Fig. 1(d)–(g). It is found that the monoclinic and tetragonal phases coexist and that the intensity of the reflection peaks is greater than the corresponding peak seen in Fig. 1(c). The intensity of the monoclinic peaks $(\bar{1}\,1\,1)_M$ and $(1\,1\,1)_M$ increases as the calcination temperature increases from 773 to 1073 K, and the crystallinity or size of the tetragonal phase is also remarkably increased. This result demonstrates that the crystallinity of the 3Y-PSZ freeze dried precursor powders increases with increasing calcinations temperature.

The average crystallite size was determined by XRD, of the tetragonal and monoclinic ZrO_2 in 3Y-PSZ freeze dried powders calcined at various temperatures for 2 h are shown in Fig. 2(a). The determination indicates that the crystallite size of tetragonal and monoclinic ZrO_2 increases from 7.25 to 18.3 nm, and 10.1 to 21.6 nm, respectively, when the

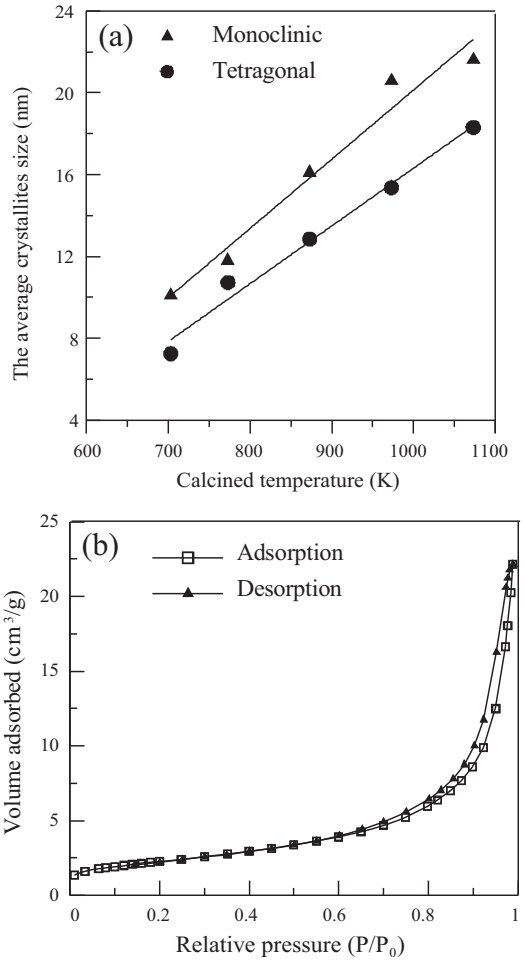

Fig. 2. (a) The average crystallite size, as determined by XRD, of the tetragonal and monoclinic ZrO_2 in 3Y-PSZ freeze dried precursor powders calcined at various temperatures for 2 h, and (b) N_2 adsorption/desorption isotherms of 3Y-PSZ freeze dried precursor powders calcined at 773 K for 2 h.

calcinations temperature increased from 703 to 1073 K. Fig. 2(b) shows the N_2 adsorption/desorption isotherms of 3Y-PSZ freeze dried precursor powders calcined at 773 K for 2 h. The curve, at a relative pressure (P/P_0) of about 0.6–0.98, has an H3-type of hysteresis loop due to the plate-like or small particle interconnects created the pores [12]. The BET specific surface area of the 3Y-PSZ freeze dried precursor powders calcinations at 703 K for 2 h is 118.42 m^2/g, which is equivalent to an average crystallite size of 8.14 nm. The crystallite sizes determined via XRD and BET agree well for the tetragonal phase while the monoclinic phase content of ZrO_2 is very small and its size, as determinate, may be omitted. The results also indicate that the powders are virtually nonagglomerated.

Moreover, in a suitably alloyed and fired ZrO_2–Y_2O_3 system, transformation from the metastable tetragonal phase to the monoclinic phase can be induced at room temperature by a mechanical force [5]. The ZrO_2–Y_2O_3 system in the range 6–12 mol% $YO_{1.5}$ from 2200 to 1700 °C which if cooled rapidly will be tetragonal at room temperature. Slow cooling results initially in the separation of tetragonal and cubic phases, and the tetragonal phase transforms to monoclinic at a lower

temperature. Thus the tetragonal phase is metastable, which is observed only on rapid cooling from high temperature [13]. In the present study, the tetragonal phase is formed and maintained when the 3Y-PSZ freeze dried powders are calcined at 673 K for 2 h. The tetragonal phase content decreases when the calcinations temperature is increased. The phase transformation of 3Y-PSZ crystallites from tetragonal to monoclinic calcined at 673–1073 K for 2 h. The intensity of the reflection *h k l* in the X-ray powder diffraction pattern of the crystal powders can be used, as proposed by Gavrie and Nicholson, to determine the tetragonal phase content [14]. When the phase transforms from tetragonal to monoclinic, the integrated intensity ratio of α_T and hence the tetragonal phase content is defined by

$$\alpha_T\ (\%) = \frac{I_T(1\,0\,1)}{I_M(\bar{1}\,1\,1) + I_M(1\,1\,1) + I_T(1\,0\,1)} \quad (3)$$

where α_T is the ratio of the tetragonal phase, I_T and I_M are the intensities of the tetragonal and monoclinic phase, respectively.

When the 3Y-PSZ freeze dried precursor powders are calcined from 673 to 1073 K for 2 h, the tetragonal ZrO_2 decreases from 100.0 to 40.6%.

The DTA/TG curves of the 3Y-PSZ freeze dried precursor powders measured at a heating rate of 5 K/min in static air are shown in Fig. 3(a). An endothermic peak at about 353 K is accompanied with a weight loss of 7% which is attributed to the evaporation of the ethanol–water solution. The weight loss at 373–703 K is attributed to the dehydration of precursors. The first exothermic peak around 550–580 K due to the formation of the tetragonal phase of ZrO_2 in the 3Y-PSZ freeze dried precursor powders. The second exothermic peak at 700 K is attributed to the tetragonal to monoclinic ZrO_2 transition. Based on the results shown in Fig. 1(c), although the quantity of the monoclinic phase is so low, but the tetragonal to monoclinic transition is still observed, and hence the exothermic peak at 700 K can be attributed to the transformation of the tetragonal to monoclinic. The absence of the monoclinic phase during the first stage of crystallization may be due to the close relation between the developing tetragonal ZrO_2 and the amorphous reactant or to the small crystallite size of $ZrO_{2\,(T)}$ [15–17].

Komissarova et al. [18] have pointed out that the DTA curves for zirconia gels show an initial endothermic peak at about 473 K followed by a strong exothermic peak at about 673 K; the latter is attributed to crystallization of tetragonal ZrO_2 from the amorphous state. According to the arguments presented by Whitney, [19] the strong exothermic peak is associated with the transformation of $[Zr_4(OH)_2O_6](OH)_2$ into the crystalline $ZrO_{2\,(T)}$ lattice [19]:

$$[Zr_4(OH)_2O_6](OH)_2 \rightarrow 4ZrO_{2\,(T)} + 2H_2O \quad (4)$$

Maiti et al. [20] have studied the kinetics and burst phenomenon in ZrO_2 transformation by DTA and have pointed out that the tetragonal–monoclinic transformation temperature in ZrO_2 is strongly affected by the change in crystallite size. The tetragonal–monoclinic transition temperature on heating from the calcinations temperature shifts to higher values with increasing crystallite size. Maiti et al. [20] have reported that on heating the tetragonal–monoclinic transformation temperature increases from 1124 to 1248 K when the crystallite size increases from 32.5 to 123.5 nm. The corresponding transition temperature depends on the size of the ZrO_2 crystallites. In the present study, the tetragonal–monoclinic transformation occurs at about 773 K, which is much lower than the results of Maiti et al. [20]. The decrease in transition temperature may be due to the fact that the initial crystallite size range of tetragonal ZrO_2 formation in 3Y-PSZ freeze dried precursor powders is suitable and causes the temperature of tetragonal–monoclinic transformation to shift downward.

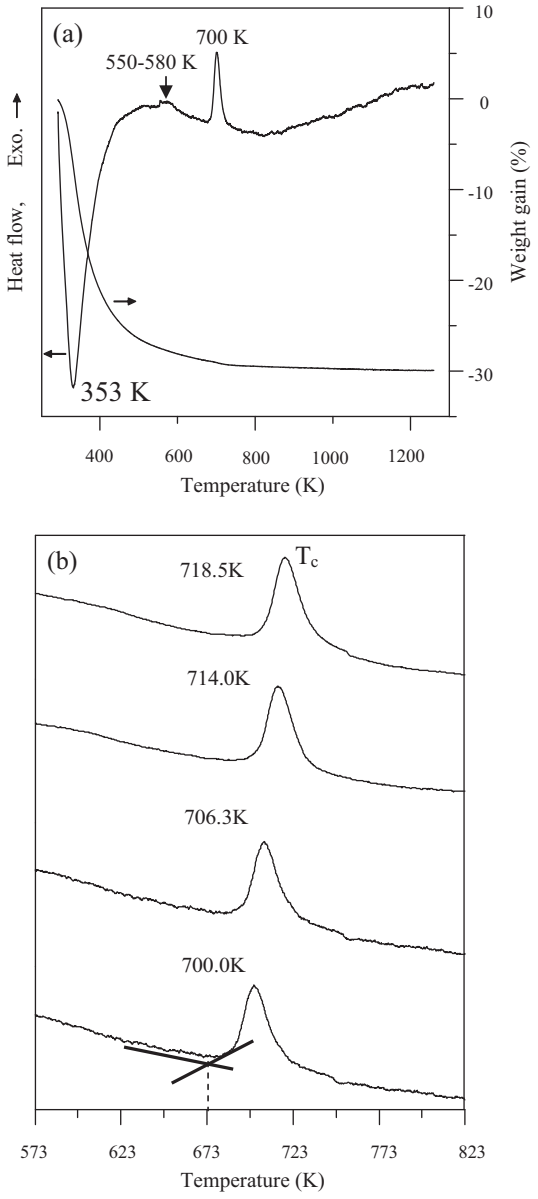

Fig. 3. (a) DTA/TG curves for 3Y-PSZ freeze dried precursor amorphous powders at heating rate of 5 K/min in air and (b) exothermic peak temperatures of 3Y-PSZ freeze dried precursor amorphous powders at heating rates of 5, 10, 20 and 30 K/min. See text for explanation.

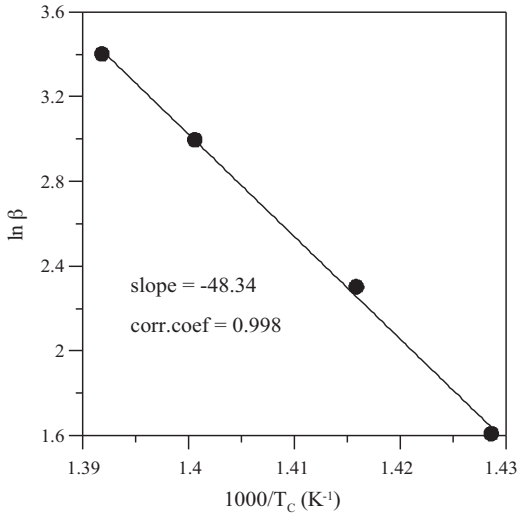

Fig. 4. Plots of ln β vs. $1000/T_c$.

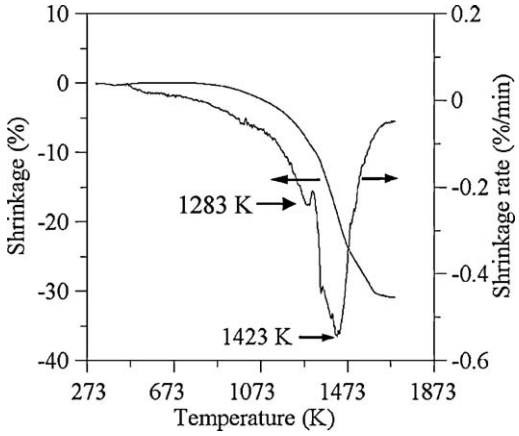

Fig. 5. Sintering curves of 3Y-PSZ freeze dried precursor powders after calcined at 773 K for 2 h via DA under a constant heating rate of 5 K/min.

3.2. Kinetics of the tetragonal ZrO_2 formation in the 3Y-PSZ freeze dried precursor powders

Fig. 3(b) shows the DTA curves for the tetragonal to monoclinic ZrO_2 transition of the 3Y-PSZ freeze dried precursor amorphous powders at the heating rates from 5 to 30 K/min. It is found that the exothermic peak for T → M transformation shifts to a high temperature when the heating rate increases. This phenomenon suggests that when the heating rate increases, the tetragonal to monoclinic transition is delayed to the high temperature side.

'The heat evolution in a small time interval is directly proportional to the number of reacting moles, namely the instantaneous reaction rate. The temperature of the exothermic peak (T_c) is dependent on the heating rate, β, according to the Arrhenius equation [21]:

$$\beta = CM \exp\left(-\frac{E_c}{RT_c}\right) \quad (5)$$

where E_c is the activation energy for crystallization, R denotes the universal gas constant, M means the number of nuclei, and C is the constant.

The Johnson–Mehl–Avrami (JMA) equation [22] can be applied to derive the non-isothermal activation energy of the tetragonal to monoclinic ZrO_2 transition in the 3Y-PSZ freeze dried precursor powders as follows:

$$\ln \beta = -\frac{E_c}{RT_c} + \ln CM \quad (6)$$

where ln CM is the constant.

From the result of the DTA curves at various heating rates, a linear relation holds between ln β and $1/T_c$ as demonstrated in Fig. 4. The line in the figure is fitted with its correlation coefficient by a polynomial method. Thus, the apparent activation energy 401.89 kJ/mol is obtained from the slope of fitting a straight line, which is larger than that of the ~70 kJ/mol of the tetragonal to monoclinic transformation for 5 wt% yttria-stabilized zirconia by electron-beam deposited coatings [23]. This result is also larger than that of 100 kJ/mol for the isothermal tetragonal-to-monoclinic transformation of a 3Y-PSZ ceramics from 343 to 403 K in water [24]. The result of the present study is also much larger than that of 22.74 kJ/mol for the isothermal tetragonal to monoclinic transformation in 3 mol% Y_2O_3–ZrO_2 ceramics [25]. Furthermore, the result of the present study is also larger than that of 231.76 kJ/mol for the crystallization of the cubic phase in 8YSZ nano-powders [6].

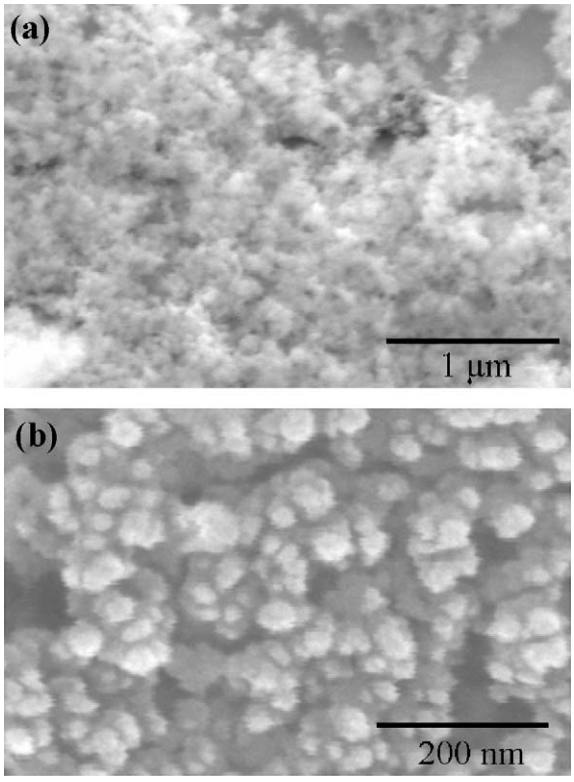

Fig. 6. SEM micrograph of 3Y-PSZ freeze dried precursor powders calcined at 773 K for 2 h.

3.3. Sintering curves for the 3Y-PSZ nanocrystallite powders

Fig. 5 shows 3Y-PSZ sintering curves for a compact of uniaxially pressed freeze dried precursor powders, previously calcined at 773 K for 2 h via DA at a constant heating rate of 5 K/min. The compact exhibits a very good sinterability, and a significant linear shrinkage of 8% is observed at about 1283 K. The final density is achieved at approximately 1623 K, by which time a total shrinkage of 32% was recorded and the density is calculated to be greater than 99% of the theoretical density. The shrinkage rate obtained by differentiating the shrinkage curve is also illustrated in Fig. 5 and indicates that the densification rate is near zero at 1623 K. There are two peaks located at 1283 and 1423 K, respectively. The maximum densification rate is found at 1423 K, demonstrating rapid low temperature sinterability of the 3Y-PSZ nanocrystallite powders. The rapid densification of 3Y-PSZ powders at low temperature can be attributed to two routes: firstly the effect of particle size [26] or surface and secondly is the reduction in lattice and grain boundary transport limited [27]. The importance of particle size in determining sintering rate can be seen in the inverse dependencies of the sintering equation on particle radius r [27]:

$$\left(\frac{x}{r}\right)^n = \frac{\text{constant}}{r^p} t \tag{7}$$

where x is the radius of the neck of particles together, the constant contains the surface tension and the relevant diffusion coefficient, n is between 2 and 6, and p is between 2 and 4.

In the present study, the crystallites size of the 3Y-PSZ nanopowder is less than 20 nm, although the 3Y-PSZ nanopowder exists as agglomerates, the size of agglomeration is still smaller than 40 nm. Hence, it is anticipated the effect of surface area of the calcined powder in densification of the sintered 3Y-PSZ compact will have a dominant effect at lower temperature.

On the other hand, grain boundary and lattice diffusion have a steeper temperature dependence and tend to dominate at higher temperature, thereby promoting further densification. Surface diffusion and evaporation–condensation have weaker temperature dependencies and often dominate at low-temperatures when reduced in lattice and grain boundary transport are limited [27]. The principle behind fast-firing [27] or rapid heating to promote densification is to limit the grain coarsening regime.

3.4. Microstructure of the 3Y-PSZ nanocrystallites

Fig. 6 shows the SEM micrograph of the 3Y-PSZ freeze dried precursor powders calcined at 773 K for 2 h. During

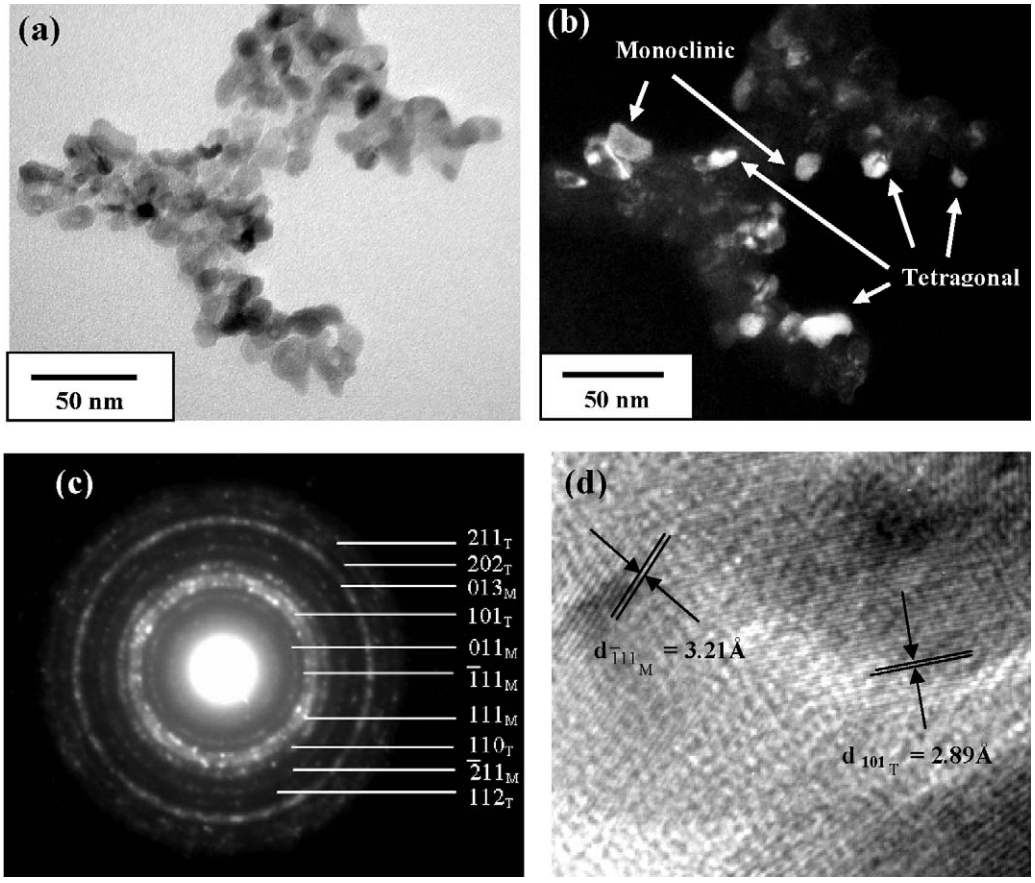

Fig. 7. TEM and HRTEM micrographs of 3Y-PSZ freeze dried precursor powders calcined at 773 K for 2 h: (a) BF image, (b) DF image shows the tetragonal and monoclinic ZrO_2, (c) corresponding ED pattern showing the monoclinic and tetragonal ZrO_2, (d) lattice image showing lattice spacings of $(\bar{1}\,1\,1)_M$ and $(1\,0\,1)_T$ ZrO_2, 3.21 Å and 2.89 Å, respectively.

calcinations, the agglomeration in nanopowders is due to the solid-state bonds necking formed between nanoparticles. The 3Y-PSZ freeze dried precursor powders are wormlike in appearance and are formed by soft agglomeration.

The bright and dark fields (BF and DF) TEM micrographs of the 3Y-PSZ freeze dried powders calcined at 773 K for 2 h are shown in Fig. 7. The BF TEM image of Fig. 7(a) shows ZrO_2 nanocrystallite clusters appearing with particle diameters ranging from 10 to 20 nm within the clusters. Fig. 7(b) shows the DF images of tetragonal and monoclinic ZrO_2, respectively, within the same clusters. The ED pattern (Fig. 7(c)) also provides evidence for the presence of the tetragonal and the monoclinic ZrO_2 in this system. The HRTEM image of Fig. 7(d) shows that the lattice spacings of $(\bar{1}\,1\,1)_M$ and $(1\,0\,1)_T$ of the monoclinic and tetragonal ZrO_2 nanocrystallites are found to be 3.21 Å and 2.89 Å, respectively. This result provides further evidence for the coexistence of the monoclinic (M) and tetragonal (T) ZrO_2 within the calcined powders. The pre-existing M-domains may well act as heterogeneous nuclei for tetragonal to monoclinic transformation.

4. Conclusions

The phase transformation kinetics of 3 mol% yttria partially stabilized zirconia (3Y-PSZ) nanocrystallites using isothermal and nonisothermal methods have been investigated. The results are concluded as follows for 3Y-PSZ freeze dried precursor powders:

The phase transformation temperature of tetragonal to monoclinic ZrO_2 determined by DTA analysis is 700 K and increases as the heating rate increases from 5 to 30 K/min. The activation energy from tetragonal ZrO_2 phase transformation to monoclinic ZrO_2 at ~700 K in 3Y-PSZ freeze dried precursor powders was determined to be 401.89 kJ/mol.

The BET specific surface area of the 3Y-PSZ freeze dried precursor powders is 118.42 m^2/g, which is equivalent to a crystallite size of 8.14 nm.

The final densification rate is at approximately 1623 K, by which time a total shrinkage of 32% was recorded and a final density above 99% of theoretical density achieved.

Both TEM and XRD examinations indicate that the tetragonal and monoclinic ZrO_2 coexist with a spherical morphology ranging from 10 to 20 nm which is in reasonable agreement with the BET determined value of 8.14 nm.

Acknowledgments

The authors wish to thank the National Science Council of Taiwan for the financial support under NSC 95-2221-E-037-007, and Prof. M.P. Hung, Prof. M.H. Hon and Mr. S.Y. Yau for offering valuable advice and suggestions on the experiments and analyses.

References

[1] N.Q. Minh, Ceramic fuel cells, J. Am. Ceram. Soc. 76 (1993) 563–588.
[2] L.W. Niedrach, Application of zirconia membrane as high-temperature pH sensors, in: N. Claussen, M. Rühle, A.H. Heuer (Eds.), Science and Technology of Zirconia II, The American Ceramic Society Inc., Columbus, Ohio, 1984, pp. 672–684.
[3] C.W. Kuo, Y.H. Lee, K.Z. Fung, M.C. Wang, Effect of Y_2O_3 addition on the phase transition and growth of YSZ nanocrystallites prepared by a sol–gel process, J. Non-Cryst. Solids 351 (2005) 304–311.
[4] C. Pascual, P. Duran, Subsolidus phase equilibria and ordering in the system ZrO_2–Y_2O_3, J. Am. Ceram. Soc. 66 (1983) 23–27.
[5] R.H.J. Hannink, P.M. Kelly, B.C. Muddle, Transformation toughening in zirconia-containing ceramics, J. Am. Ceram. Soc. 83 (2000) 461–487.
[6] C.W. Kuo, Y.H. Lee, I.M. Hung, M.C. Wang, S.B. Wen, K.Z. Fung, C.J. Shih, Crystallization kinetics and growth mechanism of 8 mol% yttria-stabilized zirconia (8YSZ) nano-powders prepared by a sol–gel process, J. Alloys Compd. 453 (2008) 470–475.
[7] Y.F. Chen, M.C. Wang, M.H. Hon, Phase transformation and growth of mullite in kaolin ceramics, J. Eur. Ceram. Soc. 24 (2004) 2389–2397.
[8] A. Goldstein, Y. Goldenberg, Boron carbide–zirconium boride in situ composites by the reactive pressureless sintering of boron carbide–zirconia mixtures, J. Am. Ceram. Soc. 84 (2001) 642–644.
[9] B.D. Cullity, second ed., Elements of X-Ray Diffraction, Addison-Wesley Publishing Company, Reading, MA, 1978, p. 81.
[10] Q. Zhu, B. Fan, Low temperature sintering of 8YSZ electrolyte film for intermediate temperature solid oxide fuel cells, Solid State Ionics 176 (2005) 889–894.
[11] H.S. Liu, T.S. Chin, L.S. Lai, S.Y. Chiu, K.H. Chung, C.S. Chang, Hydrohyapatite synthesized by a simplified hydrothermal method, Ceram. Int. 23 (1997) 19–25.
[12] G. Ertl, H. Knozinger, J. Weitkamp, Handbook of Heterogeneous Catalysis, vol. 3, 1997, WCHD-69451, Weinheim, p. 1508.
[13] H.G. Scoot, Phase relationships in the zirconia–yttria system, J. Mater. Sci. 10 (1975) 1527–1535.
[14] R.C. Gavrie, P.S. Nicholson, Phase analysis in zirconia systems, J. Am. Ceram. Soc. 55 (1972) 303–305.
[15] R.C. Gravie, Occurrence of metastable tetragonal zirconia as a crystallite size effect, J. Phys. Chem. 69 (1965) 1238–1243.
[16] R.C. Gravie, Stabilization of the tetragonal structure in zirconia microcrystals, J. Phys. Chem. 82 (1978) 218–224.
[17] H. Nishizawa, N. Yamasaki, K. Matsuoka, H. Mitsushio, Crystallization and transformation of zirconia under hydrothermal conditions, J. Am. Ceram. Soc. 65 (1982) 343–346.
[18] L.N. Komissarova, P. Yu, Z.A. Simanov, Vladimirova, Some properties of a crystal modification of ZrO_2, Zh. Neorg. Khim. 5 (1960) 687–689.
[19] E.D. Whitney, Observations on the nature of hydrous zirconia, Discuss, and Notes, J. Am. Ceram. Soc. 53 (1970) 697–698.
[20] H.S. Maiti, K.V.G.K. Gokhale, E.C. Subbarao, Kinetics and burst phenomenon in ZrO_2 transformation, J. Am. Ceram. Soc. 55 (1972) 317–322.
[21] A. Marotta, A. Buri, G.L. Valent, Crystallization kinetics of gehlenite glass, J. Mater. Sci. (1978) 2483–2486.
[22] M. Avrami, Kinetics of phase change, J. Chem. Phys. 7 (1939) 1103–1112.
[23] V. Lughi, D.R. Clarke, Low-temperature transformation kinetics of electron-beam deposited 5 wt% yttria-stabilized zirconia, Acta Mater. 55 (2007) 2049–2055.
[24] J. Chevalier, Low-temperature aging of Y-TZP ceramics, J. Am. Ceram. Soc. 82 (1999) 2150–2154.
[25] W.Z. Zhu, Effect of cubic phase on the kinetics of the isothermal tetragonal to monoclinic transformation in ZrO_2 (3 mol% Y_2O_3) ceramics, Ceram. Int. 24 (1998) 35–43.
[26] Y.M. Chiang, D.P. Birnie III, W.D. Kingery, Physical Ceramics: Principles for Ceramic Science and Engineering, John Wiley and Sons, 1997, p. 403.
[27] R.J. Brook, Fabrication principles for the production of ceramics with superior mechanical properties, Proc. Br. Ceram. Soc. 32 (1982) 7–24.